
Faculty of Science

Faculty Publications

This is a post-print version of the following article:

Mechanistic features of the copper-free Sonogashira reaction from ESI-MS

Zohrab Ahmadi, Lars P. E. Yunker, Allen G. Oliver, and J. Scott McIndoe

2015

The final publication is available at Royal Society of Chemistry via:

<https://dx.doi.org/10.1039/C5DT02889B>

Citation for this paper:

Ahmadi, Z., Yunker, L., Oliver, A., & McIndoe, J. (2015). Mechanistic features of the copper-free sonogashira reaction from ESI-MS. *Dalton Transactions*, 44(47), 20367-20375.

Mechanistic features of the copper-free Sonogashira reaction from ESI-MS

Zohrab Ahmadi,^a Lars P. E. Yunker,^a Allen G. Oliver^b and J. Scott McIndoe*^a

a. Department of Chemistry, University of Victoria, P.O. Box 3065 Victoria, BC V8W3V6, Canada.

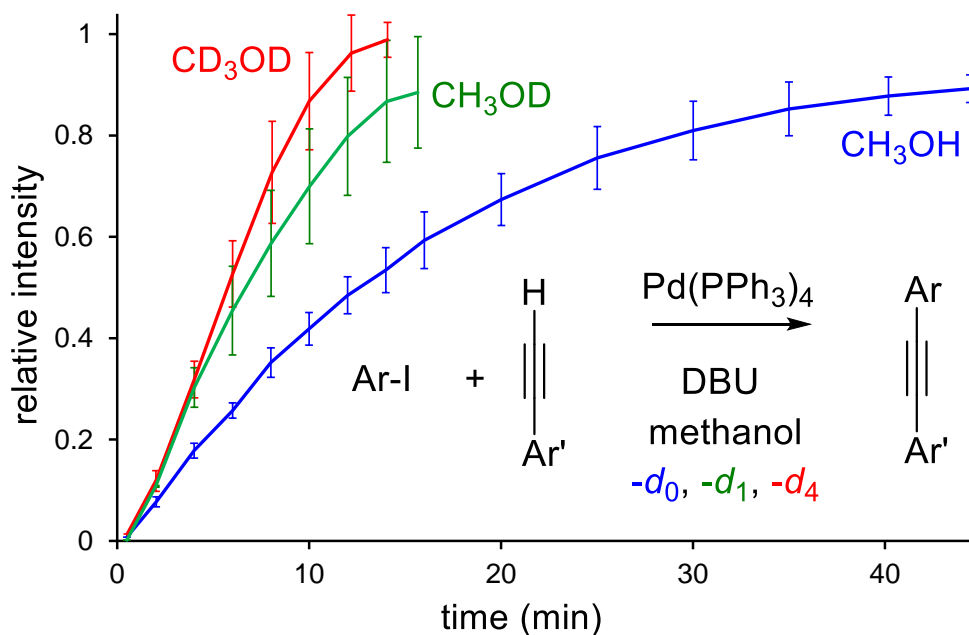
Fax: +1 (250) 721-7147; Tel: +1 (250) 721-7181; E-mail: mcindoe@uvic.ca

b. Molecular Structure Facility, Department of Chemistry and Biochemistry, University of Notre Dame, Notre Dame, Indiana 46556, United States

Keywords

Catalysis, mass spectrometry, electrospray ionization, real-time monitoring, Sonogashira coupling, Heck alkynylation

Graphical abstract



ToC text

Continuous mass spectrometric monitoring of the copper-free Sonogashira reaction reveals acceleration by stronger bases and deuterated methanol solvent.

Abstract

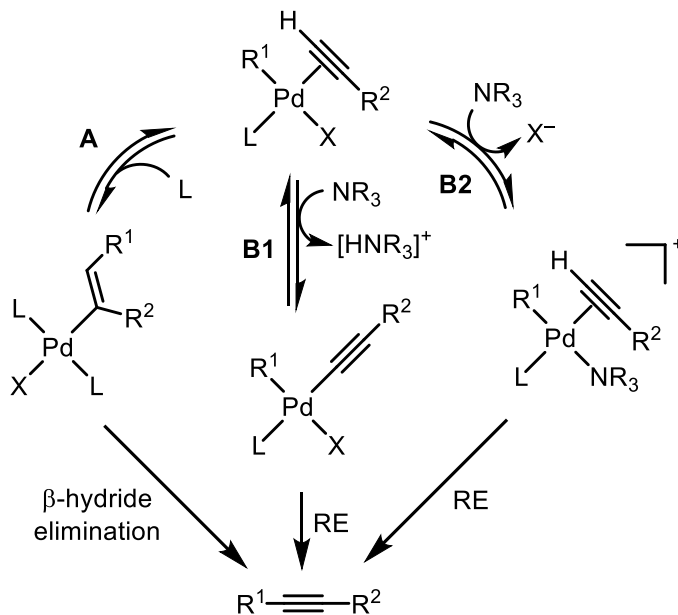
The mechanism of the Sonogashira reaction in methanol was studied in detail using pressurized sample infusion electrospray ionization mass spectrometry (PSI-ESI-MS). Several key intermediates were identified and their structures were assigned by MS/MS studies. Cationic and anionic charged-tagged substrates were employed to look into the mechanism of this reaction from variety of angles. A reverse kinetic isotope effect was observed in which the reaction rate is accelerated in deuterated solvents ($k_H/k_D = 0.6$). The reaction was found to be zero order with respect to the aryl iodide and first order with respect to the phenylacetylene. A Hammett parameter of $\rho = 1.4$ indicates that the reaction is more favorable for aryl iodides with *para* EWGs. No evidence of product inhibition, dimerization of palladium catalyst, or agglomeration were observed. However, catalyst decomposition was inferred from a non-zero intercept in the plot of catalyst loading versus reaction rate. Monitoring the reaction by PSI-ESI(-)MS on neutral and negatively charged substrates at variety of concentrations and conditions did not reveal any detectable anionic palladium complexes. Likewise no evidence of carbopalladation and relevant intermediates in the absence of a base was observed.

Introduction

The Heck alkynylation reaction was reported independently in 1975 by Heck¹ and Cassar², and involves a palladium-catalyzed carbon-carbon bond forming reaction between a terminal alkyne and an aryl or vinyl halide. Shortly thereafter, Sonogashira reported that addition of trace CuI to this reaction improved the reaction significantly, allowing reactions to be conducted at room temperature in addition to generally increasing yields. A preliminary catalytic cycle was proposed in the same report which indicated the role of CuI and suggested a mechanism with biphenylacetylene formation as the byproduct.³ Thereafter, this reaction became very popular for the synthesis of natural and biologically active products, heterocycles, dendrimers, conjugated polymers and nanostructures.⁴ Regardless of whether copper iodide is present, the coupling of a

terminal alkyne with an sp^2 carbon catalyzed by a palladium complex is most often called “Sonogashira reaction”, perhaps because Heck (a 2010 Chemistry Nobel Prize-winner) is strongly identified with the so-called “Heck reaction”, the coupling of an unsaturated halide with an alkene. However, with growing concerns of the environmental friendliness and difficulty of separation of the copper catalyst, the reaction became less popular. Also, this reaction suffers from the homocoupling of acetylene as a byproduct, which further reduced its popularity.⁵ In response to these shortcomings, a copper-free variant of the Sonogashira reaction was developed, and Nájera has recently documented advances in the Sonogashira reaction in two comprehensive reviews.^{4, 6}

In parallel to the many advances and improvements in the application of the Sonogashira reaction, considerable mechanistic work has been carried out. In all proposed mechanisms, the three standard steps of palladium cross coupling reactions are present: oxidative addition of aryl halide to the Pd catalyst, transmetallation of alkyne, and reductive elimination of the final product. The second step is called transmetallation by convention, since in many palladium-catalyzed cross coupling reactions the second coupling partner is transferred from another metal to the palladium (for example magnesium in the Kumada reaction or tin in the Stille reaction). Despite that fact that there is no second metal in the copper-free Sonogashira reaction, this term is still used. This step is the most difficult to study in the mechanism and several studies have attempted to understand how the alkyne is transferred to Pd catalyst. For transmetallation in the Sonogashira reaction, complications arise from the fact that the amines generally used in Sonogashira reaction are not strong enough to appreciably deprotonate the alkyne in solution. Therefore, deprotonation is hypothesized to occur on the metal: first coordinating in η^2 -fashion to the metal center, pulling electron density away from acetylene. This makes the terminal proton more acidic, enabling deprotonation by weaker bases,^{7, 8} a phenomenon observed for numerous different metals.⁹ Another proposed mechanism after formation of the η^2 -coordinated alkyne is carbopalladation followed by proton abstraction by the base (base-assisted β -hydride elimination) (Scheme 1).^{1, 10}



Scheme 1. Proposed pathways of transmetalation and subsequent reductive elimination of η^2 -acetylene-Pd complex: (A) Carbopalladation pathway; (B1) Deprotonation via formation of an anionic palladium complex; (B2) deprotonation via formation of a cationic complex of palladium. R^1 = aryl or vinyl; R^2 = aryl, alkenyl, alkyl or silyl; L = phosphine; X = halide; NR_3 = amine.

In an study supported by 1H and ^{31}P NMR data, Amatore and Jutand investigated the reactivity of *trans*-Pd(PPh₃)₂PhI with EtO₂CC≡CH. Regioselective carbopalladation was observed by initial formation of the *cis*-adduct of PdI(PPh₃)₂(C(CO₂Et)=CHPh) followed by *cis-trans* isomerization to make the *trans* form of this adduct.¹⁰

Ljungdahl *et al.* cast doubt on whether the carbopalladation mechanism was operating under real catalytic conditions.⁷ In that study, a product of carbopalladation was synthesized and was subjected to a typical Sonogashira catalytic reaction in the presence of phenylacetylene with and without base (excess Et₃N) to check the possibility of base-assisted *trans*-elimination and intramolecular beta hydride elimination respectively. No desired product was formed, which excluded the possibility of carbopalladation mechanism under actual reaction conditions. Having ruled out the carbopalladation mechanism, they proposed that the deprotonation mechanism was operative in catalytic conditions, and that the turnover limiting step of two competing mechanisms

depends on the electronic effects of the terminal alkyne. In addition, they observed a mechanism changeover in a Hammett study of a series of *para*-substituted terminal alkynes. It was observed that the energy required for deprotonation is decreased by electron withdrawing groups (EWG) and increased by electron donating groups (EDG). Two different pathways were proposed and supported computationally: the first when the proton of the terminal alkyne is acidic enough (with *para*-substituted EWG-substituents) to make deprotonation facile and the reaction proceeds through an anionic pathway to make a coordinatively saturated palladate complex. The second case occurs if the terminal proton is not acidic enough (*para*-substituted EDG-substituents), making base-assisted deprotonation very slow, so further activation is required to progress in the cycle and the carbopalladation mechanism will be dominant. Acting in a dual role, the base will substitute the halide initially to create an electron deficient palladium complex, and the η^2 complex can subsequently undergo deprotonation more easily.

Jutand *et al* also reported on the existence of two mechanisms.¹¹ This time different amines were shown to participate with multiple roles. It was suggested that the base initially accelerates the overall reaction by interfering in the OA step, forming the more reactive species of the type $\text{Pd}^0\text{L}(\text{amine})$. Also, secondary amines can replace the ligand (L) in *trans*- $\text{Pd}^{\text{II}}\text{L}_2(\text{Ph})(\text{X})$, being more favorable for $\text{L} = \text{AsPh}_3$ than $\text{L} = \text{PPh}_3$. However, in a computational study (which considered four major steps for this reaction including OA, *cis-trans* isomerization, deprotonation, and RE with a primary amine and $\text{Pd}(\text{PPh}_3)_4$), the amine was shown to inhibit oxidative addition by formation of stable complexes with palladium.¹² In a high-throughput kinetic study using gas chromatography, the electronic and steric effects of substrates and ligands were studied for the copper-free Sonogashira reactions by the use of Eyring and Hammett plots and supported by DFT calculations, and indicated that the aryl halide is somehow involved in the turnover limiting step.¹³ The electronic effects of *para*-substituents on the aryl iodide have been investigated with ESI-MS/MS.¹⁴ The results of this study indicated that reductive elimination is most favorable for aryl halide groups with electron donating substituents, in agreement with a theoretical study.¹⁵

ESI-MS has lent itself to the study of the organometallic catalytic mechanisms thanks to its speed, sensitivity, high dynamic range and ability to handle complex mixtures. However, neutral species are invisible in ESI process, so a permanent charge is often installed on reactants

or ligands as a probe (ensuring that the charge is electronically distanced from the reaction site).¹⁶⁻
¹⁹ Initially the utilization of ESI-MS in solution was limited to identification of short lived intermediates, especially in palladium catalyzed C-C bond forming reactions.^{14, 17, 20-25} However, the application of these approaches is being expanded to various other organometallic,²⁶⁻²⁸ organic,²⁹⁻³¹ and polymerization reactions.³² Transmetalation species in copper-, silver-, and gold-addition Sonogashira reactions was recently studied by ESI-MS by Chen *et al.*³³ In 2011, we reported the capability of ESI-MS to extract robust kinetic information in real time, in which the profile of reactants, products, and intermediates are tracked over the course of a reaction.³⁴ In this study, we employed pressurized sample infusion (PSI)^{35, 36} to introduce the reaction mixture to the ESI-MS, and our findings predictably supported three main steps: oxidative addition of the aryl halide, transmetalation, and reductive elimination. It was concluded that RE is turnover limiting at the start of the reaction, but that as the acid byproduct accumulates the reaction slows and becomes zero-order as the deprotonation equilibrium is driven backwards. Use of a stronger base ensured the reaction stayed fast and first order throughout.

In this study, we have used PSI-ESI-MS to continue to investigate the Sonogashira reaction. The phenyl acetylene was functionalized with a phosphonium group, allowing the observation of the reaction from the perspective of a different substrate. Also, the aryl iodide was charge-tagged with an anionic sulfonate substituent to allow examination of the reaction in the negative ion mode.

Experimental

All syntheses and catalytic reactions were performed under an inert atmosphere of N₂ using standard glovebox or Schlenk procedures. Except for triphenylphosphine (Alfa Aesar), triethylamine (ACP, Montreal, Quebec) and tetrakis(triphenyl)phosphine palladium (Pressure Chemical Co.) chemicals were obtained from Aldrich and used without further purification. Solvents were HPLC grade and purified on an MBraun solvent purification system. Gases were obtained from Airgas (Calgary, Canada). [4-IC₆H₄(CH₂)SO₃][PPN] and [Et₃NH]I were prepared by literature methods.^{37, 38} Syntheses of [4-IC₆H₄(CH₂)PPh₃][PF₆] and [MePPh₃][PF₆] are detailed elsewhere.³⁴ Mass spectrometric interpretation was aided with chemcalc.org online tools.³⁹

Synthesis of [4-HC₂C₆H₄(CH₂)PPh₃][PF₆]

[4-HC₂C₆H₄(CH₂)PPh₃][Br] (1 g, 1.8 mmol) and PdCl₂(PPh₃)₂ (0.06 g, 0.08 mmol) and trimethylsilylacetylene (C₅H₁₀Si) (450 μL, 3.2 mmol) and copper (I) iodide (3 mg, 0.0015 mmol) and isopropylamine (CH₃)₂CHNH₂ (700 μL, 8.5 mmol) were dissolved in 30mL mixture of toluene/methanol (70:30 v/v). The mixture was stirred at reflux for half an hour. Solution containing [4-TMSC₂C₆H₄(CH₂)PPh₃][Br] (identity was confirmed by ESI(+)-MS: *m/z* 449.2) was eluted through a silica column. Potassium carbonate (0.57 g) was dissolved in a mixture of water and methanol (25:75 v/v) and added to the filtrate. The mixture was stirred for 15 min at room temperature, generating a yellow solution with a brown precipitate. The precipitate was discarded after filtration and the solution was dried under vacuum at room temperature. 0.6 g dried brown powder was obtained and subsequently washed with water. The brown powder was dissolved in 5mL methanol and NaPF₆ (0.045g, 2.6 mmol) and stirred for one hour at room temperature. Solvent was evaporated by rotary evaporator and yellow powder was washed with water and dried under vacuum overnight. (0.4 g, 0.8 mmol, 44%). Product was recrystallized from hot methanol. (m.p. = 250 °C uncorrected). ¹H NMR (300 MHz, CDCl₃) δ = 3.05 (s, 1H), δ = 4.55, (d, 2H, J = 14 Hz), δ = 6.8 (dd, 2H, J = 2,8 Hz) δ = 7.22 (d, 2H, J = 8 Hz), δ = 7.43- 7.52 (m, 6H), δ = 7.61 (td, 6H, J = 3, 9 Hz), δ = 7.77 (td, 3H, J = 2.5, 8Hz). ³¹P NMR (300 MHz, CDCl₃) δ = 23.05(s). ESI(+)-MS *m/z* 377.1.

Mass spectrometry conditions

All mass spectra were collected on a Micromass Q-TOF *micro* mass spectrometer in positive-ion mode using pneumatically-assisted electrospray ionization. Capillary voltage: 2900 V. Cone voltage: 10 V. Extraction voltage: 0.5 V. Source temperature: 80°C. Desolvation temperature: 150°C. Cone gas flow: 100 L/h. Desolvation gas flow: 200 L/h. Collision voltage: 2 V (for MS experiments). Collision voltage: 15 - 25 V (for CID experiments). Low and high mass resolution: 10.0. MCP voltage: 2700 V.

General experimental details

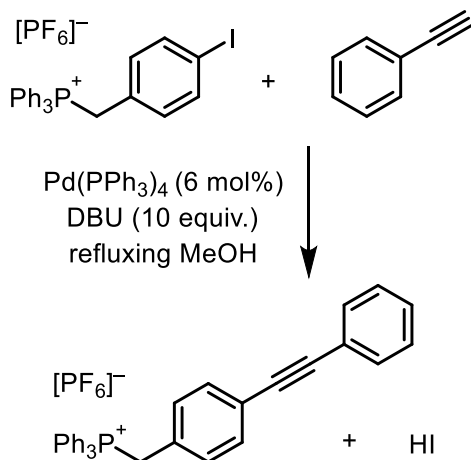
Using PSI, a solution of [I(C₆H₄)CH₂PPh₃][PF₆] (20 mL, 0.5 mM in methanol) was monitored by

ESI(+)-MS. To this solution phenylacetylene (1.3 μL , 12 μmol) and base (triethylamine or 1,8-diazabicyclo[5.4.0]undec-7-ene (DBU), 0.1 mmol) were added. 6% Pd(PPh₃)₄ (2 mL, 17 μM stock catalyst in THF) was added by syringe through the septum to initiate the reaction. The palladium tetrakis(triphenylphosphine) stock solution was stored in an inert atmosphere glovebox at -32°C between uses. Overpressure in the flask was held at 2.5 psi throughout the reaction and the temperature was held at reflux throughout. The reaction mixture was diluted online en route to the MS with methanol at 10 -20 $\mu\text{L}/\text{min}$. The diluted solution was split and flow rate to the mass spectrometer was about 0.5 $\mu\text{L}/\text{min}$. Data was processed by normalizing the abundance of each species to the total ion current attributable to species containing Ar.

Results and discussion

2.1 Reaction conditions

Scheme 2 shows our standard reaction conditions for the copper-free Sonogashira reaction, where the aryl halide bears a positively charged phosphonium tag distanced from the electronic environment of the reactive aryl ring by a methylene group. This tag provides very low detection limits and consistent intensity in the mass spectrometer due to its high surface activity. The bulky nature of the phosphonium group ensures that the ionization efficiency is largely insensitive to the structure of the ion, so the intensity of substrate and products tracks near linearly to their real concentrations. Detailed information of the nature of this tag can be found in our previous report.³⁴ Also, to reduce ion pairing, the hexafluorophosphate counterion was chosen for this charged aryl halide. The reaction conditions were optimized to bring ion intensity into the appropriate range of the instrument, and to ensure that the reaction went to completion in a reasonable amount of time (Scheme 2). The final product of this reaction was fully characterized, indicating that the phosphonium tagged aryl iodide yields the expected Sonogashira product (Figure 1).



Scheme 2: Conditions for the copper-free Sonogashira reaction with a phosphonium tagged aryl iodide as an ESI(+)-MS handle. A typical reaction involves $\text{IC}_6\text{H}_4\text{CH}_2\text{PPh}_3\text{PF}_6$ (20 ml, 0.5 mM in methanol), phenylacetylene (1.3 μL , 12 μmol), base (triethylamine or 1,8-diazabicyclo[5.4.0]undec-7-ene, DBU), 0.1 mmol), and $\text{Pd}(\text{PPh}_3)_4$ (2 mL, 17 μM stock catalyst in THF, 6%) is added by syringe to initiate the reaction.

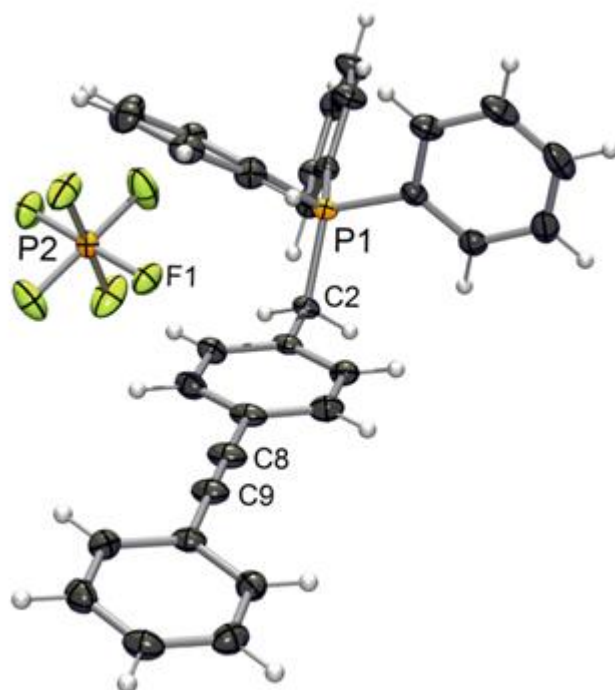


Figure 1: X-ray crystal structure of $[\text{Ph}(\text{C}_2)\text{C}_6\text{H}_4\text{CH}_2\text{PPh}_3]^+$, including the $[\text{PF}_6]^-$ counterion but not the CH_3OH of solvation. Key bond lengths: P1-C1 1.8191(15) \AA , C5-C8 1.440(2) \AA , C8-C9 1.196(2) \AA , C9-C10 1.440(2) \AA . Key bond angles: C2-C1-P1 111.27(10) $^\circ$, C9-C8-C5 178.7(2) $^\circ$, C8-C9-C10 177.78(17) $^\circ$.

An example spectrum from a typical reaction shows the relative intensities of all major tagged species is seen in Figure 2. Substrate (Ar^+I , m/z 479.1), product ($\text{Ar}^+\text{C}_2\text{Ph}$, m/z 453.2), byproduct (Ar^+H , m/z 353.2; very low intensity), and magnifications of the oxidative addition (OA) intermediate $\text{Pd}(\text{PPh}_3)_2(\text{Ar}^+)(\text{I})$ (m/z 1109.4) and transmetalated (TM) intermediates $\text{Pd}(\text{PPh}_3)_2(\text{Ar}^+)(\text{CCPh})$ (m/z 1083.3) are shown (CID experiments of the OA and TM intermediates can be found in Figure S11 and S12). The addition of an internal standard accounts for any instabilities in the ESI spray quality or fluctuations in the system (Figure 2).

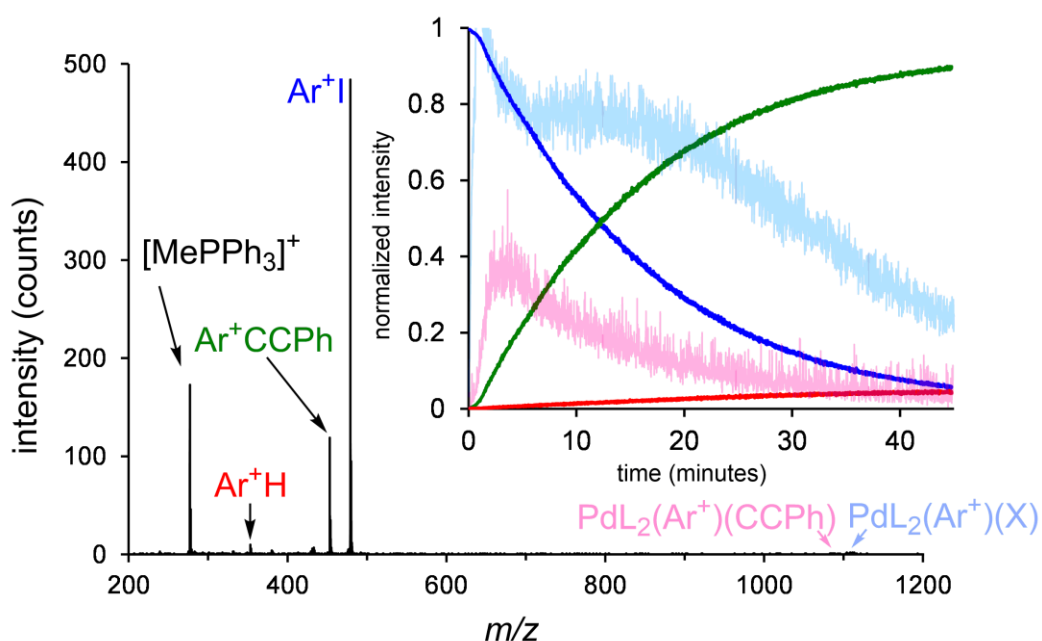


Figure 2: A single ESI(+)-MS spectrum of a standard reaction between Ar^+I and PhCCH with $\text{Pd}(\text{PPh}_3)_4$ as a catalyst ($\text{Ar}^+ = [\text{C}_6\text{H}_4\text{CH}_2\text{PPh}_3]^+$; $\text{L} = \text{PPh}_3$; $\text{X} = \text{I}^-$ or DBU). The signal at m/z 277 is the internal standard $[\text{MePPh}_3]^+$, there are no species below m/z 200 with appreciable intensity or dynamic behavior. Reaction conditions are as in Scheme 2. Inset: behavior of the species illustrated over the course of the reaction, traces are ESI(+)-MS data normalized to the total ion current. The intensities of the palladium intermediates were multiplied by 50 \times for illustrative purposes. The mass spectrum shown was collected 5 minutes after addition of catalyst.

Mechanism investigation by base alteration

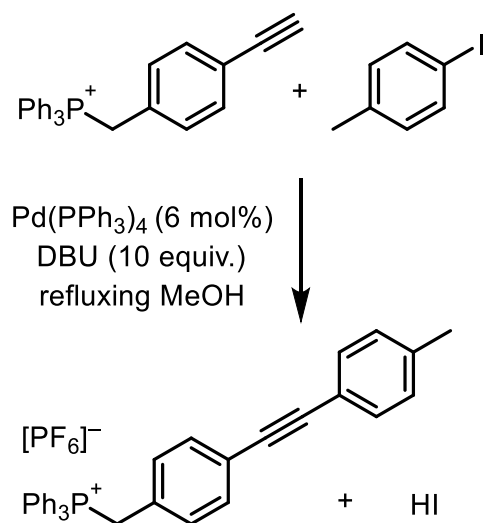
Conducting the reaction in the presence of 1,8-diazabicyclo[5.4.0]undec-7-ene (DBU) as the base results in the traces shown in Figure 2 (inset); the reaction is fast and close to first order throughout. The accumulation of $[(\text{Ph}_3\text{P})_2\text{Pd}(\text{Ar}^+)(\text{C}_2\text{Ph})]^+$ suggests that the reactions that consume it are relatively slow. An appreciable amount of $[(\text{Ph}_3\text{P})_2\text{Pd}(\text{Ar}^+)(\text{I})]^+$, $[(\text{Ph}_3\text{P})_2\text{Pd}(\text{Ar}^+)(\text{DBU})]^{2+}$ and $[(\text{Ph}_3\text{P})\text{Pd}(\text{Ar}^+)(\text{DBU})_2]^{2+}$ were also observed throughout, and these have been combined together on the basis that their abundances track closely with one another and are therefore likely to be in a fast equilibrium. Isotope pattern, m/z ratio and MS/MS supported all of these assignments (Figure SI3 and SI4). In order to see how fast the substitution occurs, ten equivalents of DBU were added to the reaction mixture in the absence of phenylacetylene at reflux in MeOH (see Figure SI5). Complete ligand replacement occurred in seconds (faster than the residence time of the solution in the tubing leading to the MS), and DBU not only replaced the iodide to form $[\text{Pd}(\text{PPh}_3)_2(\text{Ar}^+)(\text{DBU})]^{2+}$ but also PPh₃ to make $[\text{Pd}(\text{PPh}_3)(\text{Ar}^+)(\text{DBU})_2]^{2+}$. While DBU is non-nucleophilic, it can readily act as a ligand in palladium complexes.⁴⁰

It is clear that the base is playing multiple roles – not only does it deprotonate the acetylene, but can itself coordinate to the metal in place of iodide or phosphine ligand. As such, it competes with the acetylene for binding sites. Its ability to displace iodide may also make the metal center more reactive towards the acetylene and the bound acetylene more acidic. However, mono-coordinate pi-complexes tend to not be preserved during the ESI-MS process (the desolvation necessarily removes weakly bound ligands), and we did not observe any complexes involving the acetylene ligand in this binding mode.

Another experiment was performed in the absence of base to see whether any other species could be observed in the reaction mixture. We were particularly interested in any species which might suggest carbopalladation. This reaction proceeded very slowly, only forming ~1% product after 40 minutes (Figure SI6), and the only observed palladium species was $[(\text{Ph}_3\text{P})_2\text{Pd}(\text{Ar}^+)(\text{I})]^+$. This experiment suggests that carbopalladation is not a competitive mechanism under the conditions used.

Reaction with a charged terminal alkyne

Another series of experiments were conducted with a charged terminal alkyne instead of a charged aryl iodide, with the goal of identifying any alkyne-containing species that do not involve the other coupling partner. Once again a phosphonium tag was incorporated to ensure reliable surface activity in ESI(+)-MS. Scheme 3 shows a typical reaction with the charged alkyne, denoted $C_2Ar'^+$.



Scheme 3. Reaction of charged tag alkyne [*p*-HCCC₆H₄CH₂PPh₃][PF₆] (0.5 mM in 20 mL MeOH) with 1-iodo-4-methylbenzene (1.2 equivalents).

In addition to the charged alkyne and the product, three palladium intermediates were observed: $[(Ph_3P)_2Pd(C_6H_4Me)(DBU)]^+$, $[(Ph_3P)Pd(C_6H_4Me)(DBU)_2]^+$, and $[(Ph_3P)_2Pd(C_6H_4Me)(C_2Ar'^+)]^+$ (Figure 3). The behavior is highly reminiscent of the plots observed for the charged aryl iodide. The substantially greater abundance of the ions involving displacement of iodide by DBU suggests that this process is somewhat disfavoured when the complex already contains a cationic tag, perhaps explaining why the reaction is slightly accelerated.

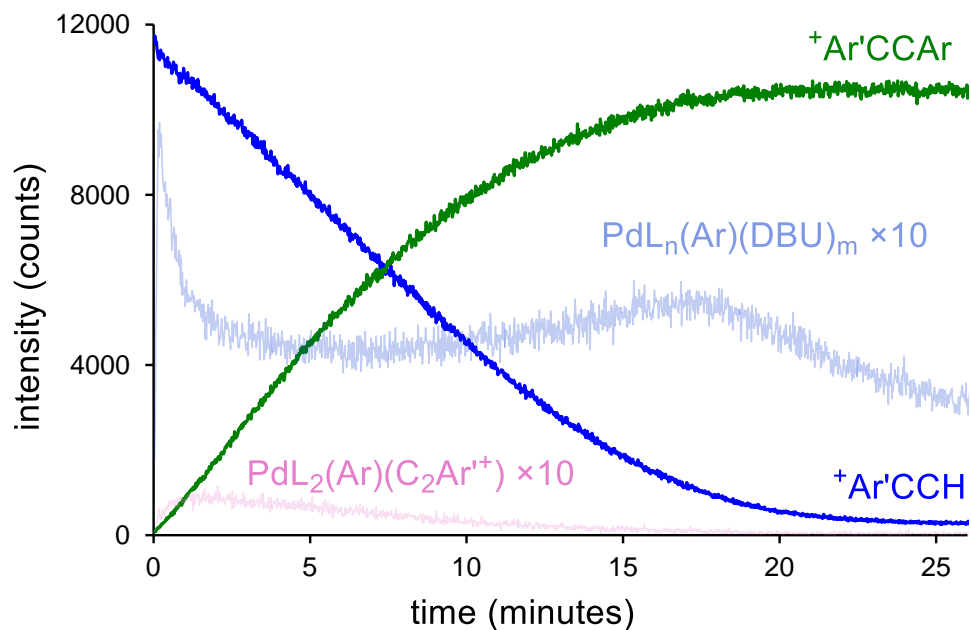


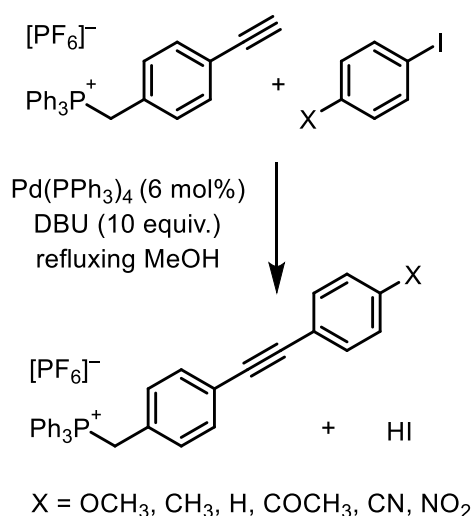
Figure 3: ESI(+)-MS intensities over time of all key species bearing the charged tag $[\text{C}_2\text{C}_6\text{H}_4\text{CH}_2\text{PPh}_3]^+$ (Ar = $\text{C}_6\text{H}_5\text{Me}$; L = PPh_3 ; X = I^- or DBU). The intensities of the palladium-containing intermediates have been multiplied by 10 for illustrative purposes. Reaction conditions are as in Scheme 3.

It is worth noting that no $[(\text{Ph}_3\text{P})_2\text{Pd}(\text{C}_2\text{Ar}^+)]^{2+}$ or $[(\text{C}_2\text{Ar}^+)_2]^{2+}$ were detected in this reaction, which are the homocoupling intermediate and product (homocoupled phenylacetylene is a common byproduct in copper assisted Sonogashira reactions).⁴¹ Judging by the lack of either of these species, it seems likely that copper is principally responsible for the homocoupling byproduct.

Multisubstrate screening by PSI-ESI-MS

Significant insight into the mechanism of a reaction can be gained by investigating the influence of various structural and electronic variables on the outcome of the reaction, and a Hammett plot is a common method of investigating the latter of the two. In order to accurately compare reactions, the conditions for each reaction must be nearly identical, which can be a logistical challenge. To avoid this issue, Kagan *et al.* introduced a “one pot multisubstrate screening” method which reacts all of the various substrates simultaneously in the same reaction vessel.^{42, 43} This method has the advantages of being faster than running many reactions separately, and the reaction conditions experienced by the different substrates are truly identical. This means

that the results of the experiment cannot be affected by bias or differing experimental conditions, the most important factor being that the catalyst handling and loading is identical. However, the rate of each product formation should be within two orders of magnitude of the all others in the same reaction, otherwise the effective catalyst concentration will not remain constant for all substrates.¹³ Here, the multisubstrate screening technique was executed with PSI-ESI-MS, allowing for a rapid and effective methodology for the study of this catalytic system. The rate of reaction of the charged alkyne with six *para*-substituted aryl iodides was studied under our standard conditions (Scheme 4).



Scheme 4: Multisubstrate screening of the charged alkyne (0.6 mM in 20 mL MeOH) with six *para*-substituted aryl iodides (2 μmol each).

The reaction was tracked beyond 90% consumption of the alkyne, and the initial linear section of each product trace (Figure 4) was subject to linear regression to extract the rate, which was then used to generate a Hammett plot (Figure 4 Inset).

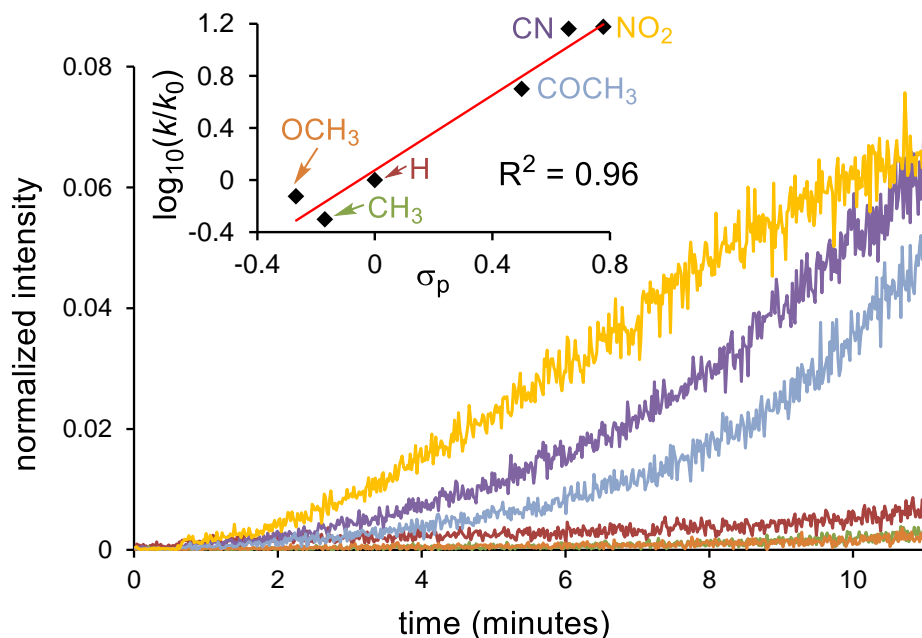


Figure 4: One pot multi-substrate reaction of the charged alkyne with a variety of *para*-substituted aryl iodides, and reaction conditions are as in Scheme 4. Traces are ESI(+)-MS data normalized to the total ion current. The initial linear portion of the reaction is highlighted to show the data which resulted in the Hammett plot. Inset: plot of $\log_{10}(k/k_0)$ vs. Hammett σ_p parameter⁴⁴ for the *para*-substituted aryl iodides shown in the traces. k is the reaction rate for the given substituent, k_0 is the reaction rate for reference substituent H.

The relative rates correlate well with σ_p values with $R^2 = 0.96$, and the positive slope of the plot ($\rho = 1.4$) indicates that the reaction is more favorable for aryl groups with electron-withdrawing substituents in the *para*-position (in agreement with the findings of Ljungdahl).⁷ It also shows the same trend as previously reported for the copper inclusive Sonogashira reaction.¹³ EWGs on the aryl group are likely stabilizing the $[(\text{Ph}_3\text{P})_2\text{Pd}(\text{C}_6\text{H}_4\text{CH}_3)(\text{C}_2\text{Ar}^{\text{r}+})]^+$ intermediate, making it less prone to reprotonation. This inference is accordance with the results of our previous mechanistic study with DBU as the base, where a CID study found a negative ρ for reductive elimination, which adds weight to the idea that transmetalation (and not reductive elimination) is turnover limiting under our reaction conditions.¹⁴

The overall rate of reaction is dependent on phenylacetylene concentration, and the reaction changes to zero order when the reaction is performed under conditions of excess phenylacetylene (Figure 5). This suggests that phenylacetylene is involved in the turnover-limiting step,

presumably the deprotonation. Under conditions of excess phenylacetylene, all three intermediates maintain a steady-state concentration before declining to the baseline once all substrate is consumed (see supporting information, Figure SI8-9).

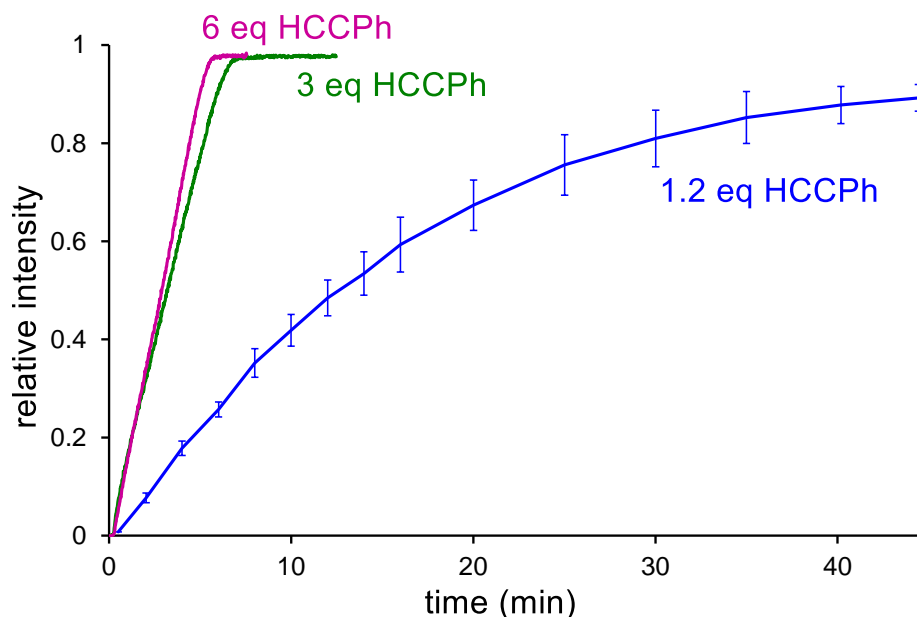


Figure 5: Appearance of product over time when using 1.2 (blue), 3 (green), and 6 (pink) equivalents of phenylacetylene. In this plot, Ar^+ (0.5 mM in 20 mL MeOH, $\text{Ar}^+ = [\text{C}_6\text{H}_4\text{CH}_2\text{PPh}_3]^+$) was reacted with phenylacetylene (1.2, 3, or 6 equivalents) in the presence of DBU (10 equivalents) and $\text{Pd}(\text{PPh}_3)_4$ (6 mol % in 2 mL THF). Traces are ESI(+)-MS data normalized to the total ion current.

Maintaining catalyst activity is an important aspect of any catalytic reaction, and there are many routes for catalyst deactivation, such as agglomeration (through formation of bi, tri to multi-nuclei until formation of agglomeration),⁴⁵ irreversible bonding to poisoning reagents (such as water or oxygen), and inhibition by compounds present in the reaction mixture. None of the reactions we have conducted have shown evidence of any species bearing more than one palladium, whereas they have been reported in some other types of cross coupling reactions as a catalyst reservoir or poisoned catalyst.⁴⁶ It is important to note that although we did not see these species, they may be present but invisible to ESI-MS if steps following dinucleation are fast (the mass of nanoparticles increases rapidly and any polynuclear species would rapidly exceed the mass range and/or signal-to-noise limits of the mass spectrometer).

Given that alkyne coordination to palladium is an assumed step in deprotonation, we wondered if the coupled alkyne product would also bind to palladium, inhibiting its ability to effect the reaction. To study this, three equivalents of biphenylacetylene were added to an otherwise standard condition reaction mixture prior to the addition of catalyst (Figure 6, Figure SI10). We did not expect to observe η^2 -biphenylacetylene-palladium species (as this weak bond is likely fragmented by the ESI process), but any effect on catalytic activity should be evident in the rate of product formation. No inhibition behavior was observed, as the rate of product formation was very similar to the reaction in the absence of biphenylacetylene.

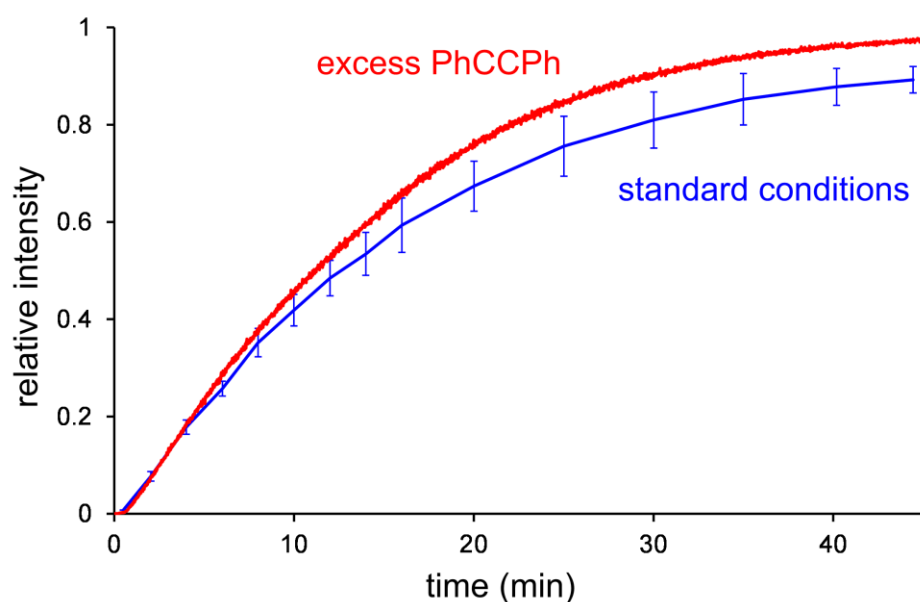


Figure 6: ESI-MS intensity data over time for the appearance of products when using excess of three equivalents biphenylacetylene (red) and standard condition (blue, an average of five runs). In this reaction, our standard conditions were used with the addition of biphenylacetylene (3 equivalents). Traces are ESI(+)-MS data normalized to the total ion current.

Kinetic isotope effects

Given the key step seemed to involve the deprotonation equilibrium, we decided to examine the reaction in deuterated methanol (CH_3OD and CD_3OD). We reasoned that if the deprotonation/reprotonation equilibrium was important, deuteration may perturb this step due to a kinetic isotope effect (KIE). This assumption was correct; the reaction was substantially *faster* in both deuterated solvents (Figure 7).

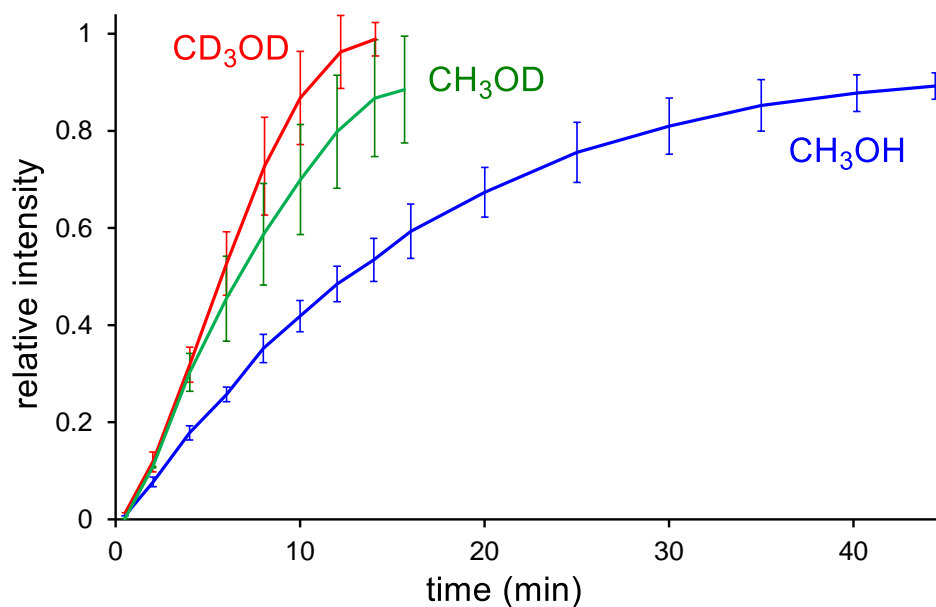


Figure 7: Overlay of Ar^+CCPh ($\text{Ar}^+ = [\text{C}_6\text{H}_4\text{CH}_2\text{PPh}_3]^+$) product build up in CH_3OH (blue), CH_3OD (green) and CD_3OD (red). Values and error bars are generated from the comparison of three, four, and five replicates for CH_3OD , CH_3OH , and CD_3OD respectively. Reaction conditions are our standard reaction conditions (Scheme 2). Traces are ESI(+)-MS data normalized to the total ion current.

These results suggest a KIE of about 0.6, with the values for CD_3OD and CH_3OD not significantly different. The most obvious conclusion is that deuteration slows reprotonation of $[(\text{Ph}_3\text{P})_2\text{Pd}(\text{C}_6\text{H}_4\text{Me})(\text{C}_2\text{Ar}^+)]^+$. An indication of whether this is true or not can be gleaned by inspection of the intermediate behaviors (Figure 8).

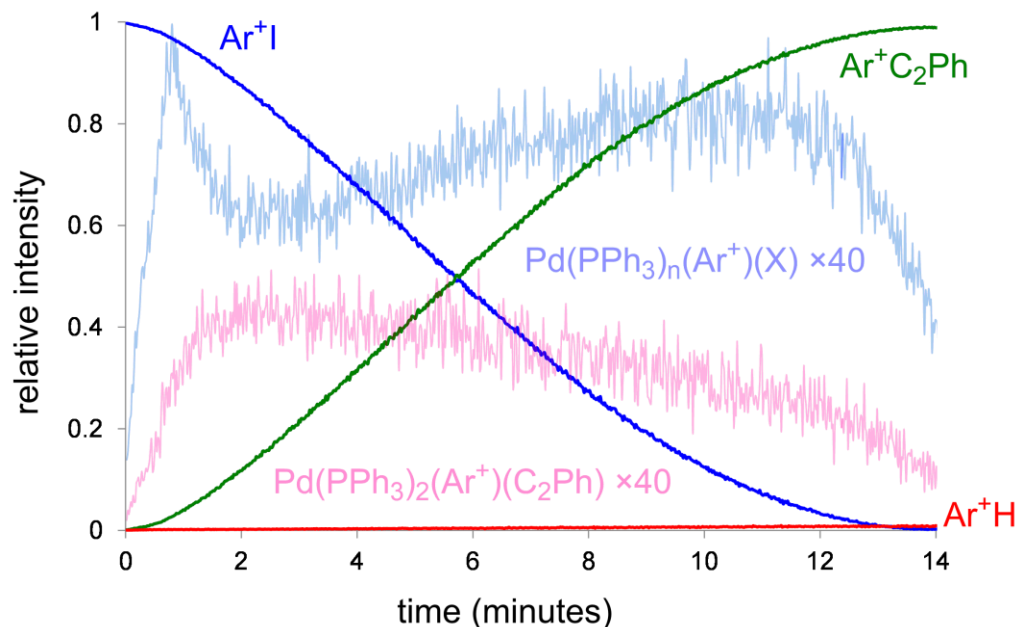


Figure 8: ESI(+)-MS over time for the intensity of all key species bearing the charged tag for the normal reaction in CD₃OD in the presence of DBU ($\text{Ar}^+ = [\text{C}_6\text{H}_4\text{CH}_2\text{PPh}_3]^+$). The reaction conditions were as in Scheme 2 with the exception of CD₃OD instead of MeOH. The intensities of the $\text{Pd}(\text{PPh}_3)_n\text{ArX}$ ($X = \text{I}^-$ or DBU) and $\text{Pd}(\text{PPh}_3)_2(\text{Ar})(\text{C}_2\text{Ph})$ have been multiplied by 40 for illustrative purposes. Traces are ESI(+)-MS data normalized to the total ion current.

Note that the abundance of $[(\text{Ph}_3\text{P})_2\text{Pd}(\text{C}_6\text{H}_4\text{Me})(\text{C}_2\text{Ar}^+)]^+$ remains high throughout the reaction, suggesting that the reactions that consume this intermediate have been slowed. There is less reason to suspect that this would be the case for the reductive elimination than for the reprotonation step. Interestingly, the reaction overall is now very fast and very clean – in particular, the amount of the ArH byproduct has now dropped below 1% and the reaction is complete within 15 minutes. This is a far cry from the initial reaction studied using NEt_3 as the base, where the reaction took close to 3 hours and produced ~20% hydrodehalogenation byproduct, Ar^+H (Figure 9).

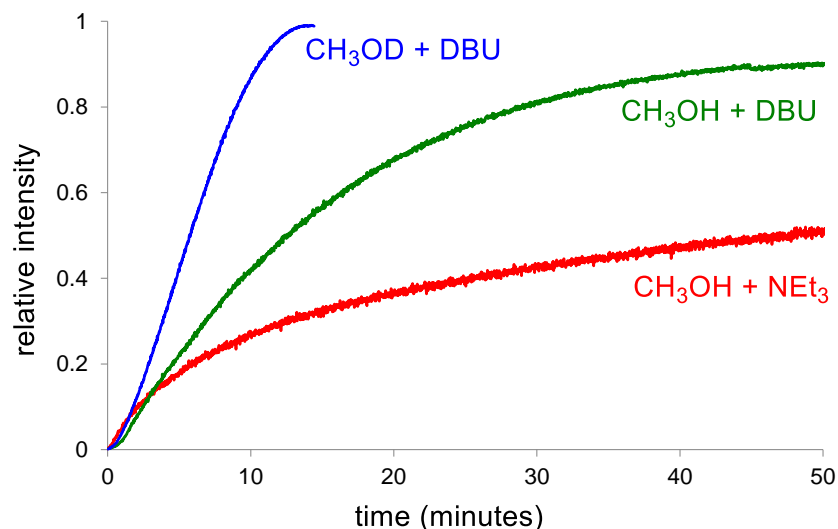


Figure 9: Comparison of ESI(+)-MS intensity data for the formation of $\text{Ar}^+\text{C}_2\text{Ph}$ ($\text{Ar}^+ = [\text{C}_6\text{H}_4\text{CH}_2\text{PPh}_3]^+$) with different bases and solvents. Each reaction uses the same catalyst loading (6 mol % relative to Ar^+) and PhCCH loading (1.2 equivalents), but varies the solvent and base as noted. The rate of Ar^+H byproduct formation (not shown) is consistent between the reactions. Each trace is ESI(+)-MS intensity data normalized to the respective total ion current.

Conclusion

Further investigation of the copper-free Sonogashira reaction using charge-tagging of substrates and real-time monitoring using PSI-ESI-MS has led to improved understanding of the factors that impinge upon the overall rate of reaction. In particular, the deprotonation/reprotonation equilibrium that leads to formation of the $\text{L}_2\text{Pd}(\text{Ar})(\text{C}_2\text{Ar}')$ intermediate (that ultimately reductively eliminates the product) seems to play a key role. Faster, cleaner reactions can be attained with the use of stronger bases (DBU rather than NEt_3), deuterated protic solvents (CD_3OD rather than CH_3OH), an excess of the phenylacetylene, and more acidic phenylacetylenes. Any one of these has a considerable effect on rate, and if several are combined, the reaction can be reduced in time from hours down to minutes. These improvements are significant as the rate of formation of the undesirable hydrodehalogenation byproduct is less affected, and so the reaction not only becomes faster but also considerably cleaner.

Acknowledgements

JSM thanks NSERC for operational funding (Discovery and Discovery Accelerator Supplements), and CFI, BCKDF and the University of Victoria for infrastructural support.

References

1. H. A. Dieck and F. R. Heck, *J. Organomet. Chem.*, 1975, **93**, 259-263.
2. L. Cassar, *J. Organomet. Chem.*, 1975, **93**, 253-257.
3. K. Sonogashira, Y. Tohda and N. Hagihara, *Tetrahedron Lett.*, 1975, **16**, 4467-4470.
4. R. Chinchilla and C. Najera, *Chem. Soc. Rev.*, 2011, **40**, 5084-5121.
5. K. J. Siemsen, J. E. Bernard, A. A. Madej and L. Marmet, *J. Mol. Spectrosc.*, 2000, **199**, 144-145.
6. R. Chinchilla and C. Najera, *Chem. Rev.*, 2007, **107**, 874-922.
7. T. Ljungdahl, T. Bennur, A. Dallas, H. Emtenas and J. Martensson, *Organometallics*, 2008, **27**, 2490-2498.
8. A. Soheili, J. Albaneze-Walker, J. A. Murry, P. G. Dormer and D. L. Hughes, *Org. Lett.*, 2003, **5**, 4191-4194.
9. S. Fujimori, Kn, ouml, T. F. pfel, P. Zarotti, T. Ichikawa, D. Boyall and E. M. Carreira, *Bull. Chem. Soc. Jpn.*, 2007, **80**, 1635-1657.
10. C. Amatore, S. Bensalem, S. Ghalem and A. Jutand, *J. Organomet. Chem.*, 2004, **689**, 4642-4646.
11. A. Tougeri, S. Negri and A. Jutand, *Chem.-Eur. J.*, 2007, **13**, 666-676.
12. L. Sikk, J. Tammiku-Taul and P. Burk, *Organometallics*, 2011, **30**, 5656-5664.
13. M. R. an der Heiden, H. Plenio, S. Immel, E. Burello, G. Rothenberg and H. C. J. Hoefsloot, *Chem.-Eur. J.*, 2008, **14**, 2857-2866.
14. K. L. Vikse, M. P. Woods and J. S. McIndoe, *Organometallics*, 2010, **29**, 6615-6618.
15. J. J. Low and W. A. Goddard, *J. Am. Chem. Soc.*, 1986, **108**, 6115-6128.
16. C. Adlhart, C. Hinderling, H. Baumann and P. Chen, *J. Am. Chem. Soc.*, 2000, **122**, 8204-8214.
17. A. O. Aliprantis and J. W. Canary, *J. Am. Chem. Soc.*, 1994, **116**, 6985-6986.
18. D. J. F. Bryce, P. J. Dyson, B. K. Nicholson and D. G. Parker, *Polyhedron*, 1998, **17**, 2899-2905.
19. C. Decker, W. Henderson and B. K. Nicholson, *J. Chem. Soc. Dalton*, 1999, DOI: 10.1039/a906010c, 3507-3513.
20. M. A. Aramendia, F. Lafont, M. Moreno-Manas, R. Pleixats and A. Roglans, *J. Org. Chem.*, 1999, **64**, 3592-3594.
21. K. Bock, J. E. Feil, K. Karaghiosoff and K. Koszinowski, *Chem.-Eur. J.*, 2015, **21**, 5548-5560.
22. C. Markert, M. Neuburger, K. Kulicke, M. Meuwly and A. Pfaltz, *Angew. Chem. Int. Edit.*, 2007, **46**, 5892-5895.
23. C. Raminelli, M. H. G. Precht, L. S. Santos, M. N. Eberlin and J. V. Comasseto, *Organometallics*, 2004, **23**, 3990-3996.
24. L. S. Santos, G. B. Rosso, R. A. Pilli and M. N. Eberlin, *J. Org. Chem.*, 2007, **72**, 5809-5812.
25. K. L. Vikse, Z. Ahmadi and J. S. McIndoe, *Coordin. Chem. Rev.*, 2014, **279**, 96-114.
26. E. Crawford, T. Lohr, E. M. Leitao, S. Kwok and J. S. McIndoe, *Dalton Trans.*, 2009, DOI: 10.1039/b913492a, 9110-9112.

27. C. Iacobucci, S. Reale, J. F. Gal and F. De Angelis, *Angew. Chem. Int. Edit.*, 2015, **54**, 3065-3068.
28. J. W. Luo, A. G. Oliver and J. S. McIndoe, *Dalton Trans.*, 2013, **42**, 11312-11318.
29. V. G. Santos, M. N. Godoi, T. Regiani, F. H. S. Gama, M. B. Coelho, R. O. M. A. de Souza, M. N. Eberlin and S. J. Garden, *Chem.-Eur. J.*, 2014, **20**, 12808-12816.
30. J. A. Willms, R. Beel, M. L. Schmidt, C. Mundt and M. Engeser, *Beilstein J. Org. Chem.*, 2014, **10**, 2027-2037.
31. R. L. Stoddard, J. W. Luo, N. van der Wal, N. F. O'Rourke, J. E. Wulff and J. S. McIndoe, *New J. Chem.*, 2014, **38**, 5382-5390.
32. J. J. Haven, J. Vandenberg and T. Junkers, *Chem. Commun.*, 2015, **51**, 4611-4614.
33. R. J. Oeschger, D. H. Ringger and P. Chen, *Organometallics*, 2015, DOI: 10.1021/acs.organomet.5b00491.
34. K. L. Vikse, Z. Ahmadi, C. C. Manning, D. A. Harrington and J. S. McIndoe, *Angew. Chem.*, 2011, **123**, 8454-8456.
35. K. L. Vikse, Z. Ahmadi, J. Luo, N. van der Wal, K. Daze, N. Taylor and J. S. McIndoe, *Int. J. Mass Spectrom.*, 2012, **323-324**, 8-13.
36. L. P. E. Yunker, R. L. Stoddard and J. S. McIndoe, *J. Mass Spectrom.*, 2014, **49**, 1-8.
37. J. G. Chen, V. Suryanarayanan, K. M. Lee and K. C. Ho, *Sol. Energ. Mat. Sol. C.*, 2007, **91**, 1432-1437.
38. S. F. Liu, C. Dockendorff and S. D. Taylor, *Org. Lett.*, 2001, **3**, 1571-1574.
39. L. Patiny and A. Borel, *J. Chem. Inf. Model.*, 2013, **53**, 1223-1228.
40. M. G. Burgess, M. Naveed Zafar, S. T. Horner, G. R. Clark and L. James Wright, *Dalton Trans.*, 2014, **43**, 17006-17016.
41. J. H. Li, Y. Liang and Y. X. Xie, *J. Org. Chem.*, 2005, **70**, 4393-4396.
42. X. Gao and H. B. Kagan, *Chirality*, 1998, **10**, 120-124.
43. T. Satyanarayana and H. B. Kagan, *Adv. Synth. Catal.*, 2005, **347**, 737-748.
44. C. Hansch, A. Leo and R. W. Taft, *Chem. Rev.*, 1991, **91**, 165-195.
45. M. Tromp, J. R. A. Sietsma, J. A. van Bokhoven, G. P. F. van Strijdonck, R. J. van Haaren, A. M. J. van der Eerden, P. W. N. M. van Leeuwen and D. C. Koningsberger, *Chem. Commun.*, 2003, DOI: 10.1039/b206758g, 128-129.
46. R. S. Paton and J. M. Brown, *Angew. Chem. Int. Edit.*, 2012, **51**, 10448-10450.